

## Hot holes in naphthalene: High, electric-field-dependent mobilities

Wilhelm Warta and Norbert Karl

*Physikalisches Institut der Universität Stuttgart, D-7000 Stuttgart 80,  
Pfaffenwaldring 57, Federal Republic of Germany*

(Received 9 October 1984)

Intrinsic time-of-flight hole mobilities ( $\mu^+$ ) were obtained in naphthalene single crystals down to 4.2 K. Between 300 and 150 K the tensor component  $\mu_{aa}^+$  increases with decreasing temperature  $T$ , obeying a  $\mu \propto T^n$  dependence, with  $n = -2.9$ . At low temperature the hole transport becomes non-linear (sub-Ohmic) with the hole velocity tending to saturate with increasing electric field,  $E$ , at about  $2 \times 10^6$  cm/s. The highest experimental  $\mu_{aa}^+$  (obtained at the lowest  $E$  which allowed the observation of a distinct hole transit pulse) was  $400 \text{ cm}^2/\text{Vs}$  at 10 K and 3 kV/cm. It will be shown that the low-temperature results can be understood in terms of a standard band-model description, whereas the continuation of the experimental temperature-dependence law ( $\mu \propto T^n$ ) (for both holes and electrons) into the high-temperature regime remains a problem for future theoretical work. Electron transits were obtained down to 22.5 K [ $\mu_{aa}^-$  (22.5 K) =  $24.5 \text{ cm}^2/\text{Vs}$ ]. No field dependence of the electron mobility was detected.

### I. INTRODUCTION

Charge-carrier mobilities  $\mu$  in purely van der Waals-bonded organic molecular crystals were first measured by Kepler<sup>1</sup> and LeBlanc,<sup>2</sup> who introduced the time-of-flight method into the organic materials field. For years, reported experimental hole and electron mobilities in crystals of aromatic molecules, such as anthracene, naphthalene, and pyrene, ranged about  $\mu = 1 \text{ cm}^2/\text{Vs}$ ; higher values, such as  $\mu^+ = 12\text{--}18 \text{ cm}^2/\text{Vs}$ , obtained for *p*-diiodobenzene in the temperature range 250–300 K by Schwartz *et al.*,<sup>3</sup> and  $\mu^- = 5 \text{ cm}^2/\text{Vs}$  obtained for phenothiazine (cf. the compilation in the review article by Karl<sup>4</sup>), were the exception. The temperature range was usually limited to  $T \geq 200$  K because of severe deep-trapping effects occurring at lower temperatures. The first successful measurement reaching liquid N<sub>2</sub> temperature was reported by Karl and Probst, cf. Karl<sup>4</sup> and Probst and Karl.<sup>5</sup> Surprisingly, the electron mobility  $\mu_{c^*c^*}^-$  in anthracene turned out to be essentially temperature independent over an interval of nearly 300 K in these measurements, amounting to  $0.4 \text{ cm}^2/\text{Vs}$ .

A mobility which strongly increased with decreasing temperature, reaching  $\mu^+(120 \text{ K}) = 55 \text{ cm}^2/\text{Vs}$ , was found in durene by Burshtein and Williams.<sup>6</sup> While the existence of high mobilities in durene was confirmed,<sup>7</sup> still higher values were measured for another compound by Stehle and Karl,<sup>8</sup> who found in perylene crystals a maximum value of  $\mu^- = 100 \text{ cm}^2/\text{Vs}$  at 30 K, and also reported at the same time the lowest temperature at which a distinct macroscopic carrier transit was observed up to now (namely 14 K, where, however, the mobility,  $\mu = 0.8 \text{ cm}^2/\text{Vs}$ , was no longer "microscopic" but multiple-shallow-trapping controlled). The previous record for a low-temperature "microscopic" (i.e., not shallow-trap-limited) mobility,  $\mu_{c^*c^*}^-$  (naphthalene, 31 K) =  $2.2 \text{ cm}^2/\text{Vs}$ , was held by Schein and McGhie.<sup>9</sup> These authors concluded from their measurements the first observation of a

"hopping-to-band" transition, occurring for naphthalene at about 100 K, since the nearly-temperature-independent  $\mu_{c^*c^*}^-$  obtained at the higher temperatures (which resembled the  $\mu_{c^*c^*}^-$  behavior in anthracene) started to rise exponentially below 100 K.

Schein and McGhie<sup>10</sup> raised the question whether a possible electric field dependence of the charge-carrier mobilities might shed some light on the underlying transport mechanism. They, in turn, performed mobility experiments for electrons in naphthalene in which they extended the electric field strength up to the highest electric fields applicable before dielectric breakdown. These measurements were confined to the low-mobility  $c^*$  direction. No effect on the electron mobility was observed for  $E \leq 170 \text{ kV/cm}$  at 160 K. A similar experiment was performed by Nakano and Maruyama<sup>11</sup> with anthracene. These authors used still higher field strengths and, for the first time, reported an electric field dependence of the electron mobility  $\mu_{c^*c^*}^-$  for  $E \geq 180 \text{ kV/cm}$  at 140 K. The effect was not very pronounced (30% at the highest field, 274 kV/cm) and was questioned<sup>12</sup> since the authors used insulating foils between the crystal and the metal electrodes, which might have nonlinearly reduced the actual field in the crystal sample because of unforeseeable space-charge effects in the foils at these extremely high field strengths. Indeed, this doubt was supported recently by Schein.<sup>13</sup> Extensive experiments, performed without insulating foils, exhibited no electric field dependence on  $\mu_{c^*c^*}^-$  up to 280 kV/cm at 140 K.

The first successful measurement of a pronounced field dependence of charge-carrier mobilities has been obtained by our group: In contrast to the previous attempts, it seemed more promising to us to search for a field dependence at higher mobilities and lower temperatures. Development of improved ultrapurification and crystal-treatment techniques led us to our final success, which will be described in this paper for naphthalene and in a planned forthcoming paper by Stehle and Karl for perylene.

The new naphthalene results have two characteristics:

(i) Very high hole mobilities. In the temperature range 40–4.2 K the experimental hole mobilities  $\mu_{aa}^+$  exceed 100  $\text{cm}^2/\text{Vs}$  and reach a maximum value of 400  $\text{cm}^2/\text{Vs}$ , which is limited by experimental restrictions only.

(ii) Electric field dependence of the mobilities. A strong decrease of these high mobilities with increasing electric field is clearly established; a non-Ohmic behavior is distinguishable for electric fields  $E \geq 10 \text{ kV/cm}$  at  $T \leq 35 \text{ K}$ . At lower temperatures, hole velocities  $v_d$  even tend to saturate with field at  $v_d = 1.8 \times 10^6 \text{ cm/s}$ .

These results can be understood in a band-type transport model, taking into account acoustic and generative optical-phonon scattering and band nonparabolicity.

## II. EXPERIMENTAL TECHNIQUE

### A. Sample preparation

Ultrapurified naphthalene was obtained as described in the literature (cf. Ref. 14). We selected the pure central fraction of the zone-refined ingot (obtained after zone refining of potassium-treated material) according to the liquid-He fluorescence spectra<sup>15</sup> (absence of  $\beta$ -methyl-naphthalene) and transferred it into a separate Pyrex tube for crystal growth by the Bridgman technique (cf. Ref. 14). The crystal was removed from the ampoule by loosening it from the ampoule wall with a solvent. Its initial triplet-exciton lifetime, determined as described before,<sup>14,15</sup> amounted to 320 ms, and tended to increase with time due to crystal annealing. Several differently oriented crystal slices were cut off with a thread saw (equipped with a thin cotton thread, wetted by a cyclohexane-xylene mixture) by dissolution rather than by mechanical abrasion. We were able to improve this cutting procedure such that no further polishing was necessary, thus avoiding the introduction of additional lattice defects. The crystal slices were left a few weeks at room temperature between thin glass cover slides and under saturated naphthalene-vapor atmosphere for thermal annealing. The exact crystallographic orientation of each sample was determined by Laue-live methods<sup>16</sup> after the electrical measurements were finished. With  $\mathbf{N}$  designating the plate normal, the orientational angles of the specimen which gave the results represented in the figures were  $\angle(\mathbf{N}, \mathbf{a}) = 6.6^\circ$ ,  $\angle(\mathbf{N}, \mathbf{b}) = 86.4^\circ$ , and  $\angle(\mathbf{N}, \mathbf{c}') = 96.6^\circ$ ; the crystal thickness amounted to 1.01(1) mm. The crystallographic  $\mathbf{a}$  direction was chosen for several reasons: (I) lying in the  $a$ - $b$  plane, it is a direction of strong interactions in the molecular layers, (II) the electron mobility exhibits no abnormal behavior in this direction [in contrast to  $\mu_{bb}$  (Ref. 17) and  $\mu_{c^*c^*}$  (Ref. 9)], and (III) the electron- and hole-mobility tensors that rotate to some extent with temperature about [010] tend to approach [100] as one principal-axis direction at low temperature. The tensor properties will be the subject of a planned, separate publication.

### B. Time-of-flight method

The crystal slices were sandwiched between a metal rear electrode and a semitransparent front electrode which

were gently pressed against the crystal by a soft spring. The sample holder was inserted into a continuous-flow He cryostat (model CF204, Oxford Instruments, with a DTC-2 temperature controller); He gas was used for heat exchange, and precise temperature calibration was performed in a separate experiment with a calibrated carbon resistor replacing the crystal sample. Charge carriers of both signs were optically generated close to one crystal surface by strongly absorbed ( $\lambda = 249 \text{ nm}$ ) light pulses of full width at half maximum (FWHM) 8 ns duration from a krypton-fluoride excimer laser (Lambda Physik model EMG 102).

Electric pulses, caused by charge carriers drifting in the applied electric field  $E$  across the entire sample, were picked up in the current mode across an external resistor  $R$  (selectable in the range 50  $\Omega$ –20  $\text{k}\Omega$ ) either by a fast field-effect-transistor (FET) probe (Tektronix, model P6201) or, if the required frequency response allowed for it, by a slower, lower-noise cathode follower plus preamplifier (Tektronix, models P170CF + 1121). Signals were displayed on a fast real-time oscilloscope (Tektronix, model 7104 with 7A29 Y-amplifier and 7B15 time base), in the single-pulse mode, and photographed. Charge-carrier transit times as a function of temperature and applied electric field were evaluated from the arrival-time kinks in the drift-current pulses (cf. Ref. 1). Measurements were taken in the temperature range 300–4.2 K. Starting from 300 K the temperature was reduced in steps of 10 K until 80 K was reached, and then in steps of 5 K. At selected temperatures the applied electric field, poled either for the observation of electron or hole transits, was varied over the experimentally accessible field range. This range was limited to 3  $\text{kV/cm}$  at low fields since the transit kink was obscured by deep trapping and noise below; the high-field limit was dictated by electric breakdown of the heat-exchange He gas at a voltage corresponding to a field of  $E \geq 14.5 \text{ kV/cm}$  across the sample.

## III. EXPERIMENTAL RESULTS

At room temperature, drift-current pulses from carriers of both signs displayed essentially no influence of deep trapping; the estimated deep-trapping lifetime for both signs was  $\tau_D \geq 100 \mu\text{s}$ . Below 80 K the *electron* lifetime decreased rapidly to about 500 ns at 25 K. Below 23 K it became appreciably shorter than the transit time, thus limiting the temperature range useful for the observation of a transit. Deep-trapping influence on *hole* transits was even more pronounced in an intermediate temperature range, where the lifetime fell from 2.5  $\mu\text{s}$  (at 100 K) to 500 ns (at 70 K). However, due to the fact that this fast decline slowed down towards lower temperatures ( $\tau_D$  was still 100 ns at 25 K, and 70 ns and more, depending on the electric field strength, at 4.2 K), the concomitant steep rise of the hole mobilities (and hence decrease of the transit time) was able to overcompensate for the trapping competition: Thus it turned out to be feasible to record hole transits down to 4.2 K, a temperature limit which was solely set by the cryostat. In Fig. 1(a) we display a representative hole-transit pulse at 4.2 K; in Fig. 1(b), an electron-transit pulse at 30 K.

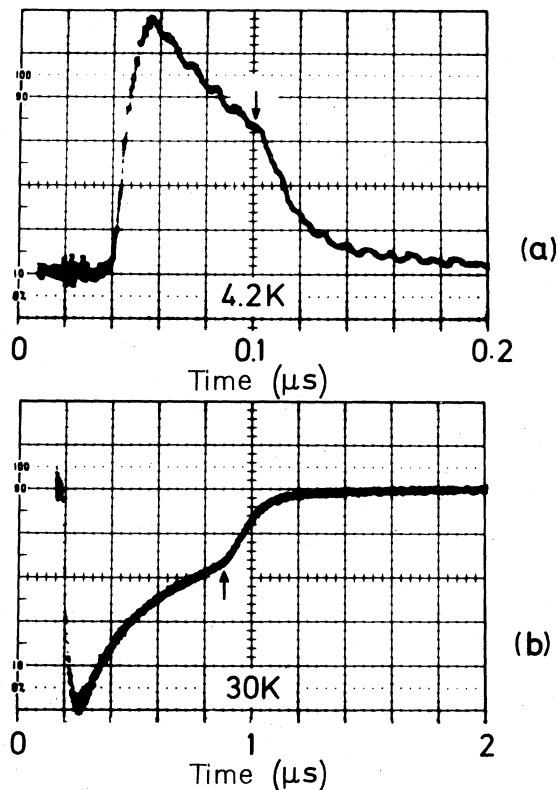


FIG. 1. Typical (a) hole and (b) electron drift current pulses. The experimental parameters are (a)  $T=4.2$  K,  $E=12$  kV/cm,  $L=1.01$  mm; ordinate scale,  $13.2 \mu\text{A}$  (per major) division, equivalent to  $\sim 40 \mu\text{A}/\text{cm}^2$  per division. (b)  $T=30$  K,  $E=10$  kV/cm,  $L=1.01$  mm; ordinate scale,  $6.6 \mu\text{A}$  (per major) division, equivalent to  $\sim 20 \mu\text{A}/\text{cm}^2$  per division. The arrival-time kinks are marked by an arrow.

In a low-symmetry crystal such as naphthalene (monoclinic, space group  $P2_1/a$ ) the relation between the measured transit time and the mobility is as follows: With  $E_N$  designating the electric field in the sample, which for the geometry used, is parallel to the normal  $\mathbf{N}$  to the crystal plate under consideration, the charge-carrier velocity component observed is the projection of  $\mathbf{v}$  on  $\mathbf{N}$ ,  $\mathbf{v} \cdot \mathbf{N} = L/t$  (where  $L$  is the crystal thickness,  $t$  the transit time, and  $|\mathbf{N}| = 1$ ). The mobility is calculated, as usual, as  $\mu_{NN} = v_N/E_N$ , the ratio of the vector component of the velocity parallel to the electric field to the magnitude of the field.  $\mu_{NN}$  is the "tensor property parallel to the given direction  $\mathbf{N}$ ," which, in general, is a linear combination of all tensor components.

The experimental mobility results are plotted in a  $\log\mu$ -versus- $\log T$  graph in Fig. 2. Within the electric field range used, field-independent mobilities, represented by solid dots, were observed in the higher-temperature regime. Below 40 K, however, and correlated with mobilities  $\geq 100 \text{ cm}^2/\text{Vs}$ , hole mobilities began displaying a marked field dependence which became more pronounced with decreasing temperature. (See Note added in proof.) A few examples of the set of results obtained for various fields are represented by open symbols, different for each field strength.

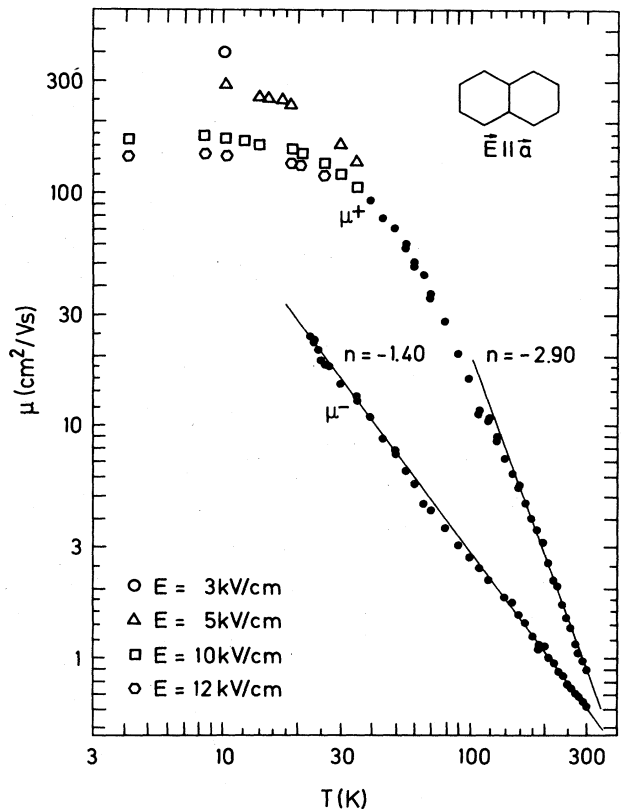


FIG. 2. Electron and hole mobilities in ultrapure naphthalene (for the applied electric field  $E$  and the detected velocity component  $v_N$ , both approximately parallel to the crystallographic  $a$  direction) vs temperature, log-log plot. At low temperatures the mobilities are electric field dependent. The solid lines indicate a  $T^n$  power-law temperature dependence with exponents  $n$  as indicated in the figure. (This figure was presented at the 10th Molecular Crystal Symposium, 20–24 Sept. 1982, St. Jovite, Canada, in a post-deadline poster.)

In the higher-temperature, field-independent mobility regime a power-law dependence of the mobilities on temperature,  $\mu \propto T^n$ , is obtained for both holes and electrons, with  $n = -2.9$  and  $-1.4$ , respectively.

In order to gain more insight into the lower-temperature field dependence, we have plotted in Fig. 3 the experimental charge-carrier drift velocities  $v_d = v_N = L/t$  as a function of the electric field for several selected sample temperatures as parameters. In this kind of graph a field-independent mobility (corresponding to a situation where Ohm's law is fulfilled) would show up as a straight line through the origin with slope  $\mu = v_d/E$ . This is approximately so only for higher-temperature mobilities, e.g., the 100-K mobilities drawn in the figure. At 31 K a slight (sublinear) deviation (although still near the experimental uncertainty) begins to appear for the lowest useful fields; at 14 kV/cm, however,  $v_d$  is already a factor of 2 lower than what would have been expected with a straight-line extrapolation from the origin through the lowest-field experimental point. Below 12 K the drift velocity tends to become almost field independent (saturated), ranging near  $1.8 \times 10^6 \text{ cm/s}$ . Further decrease of

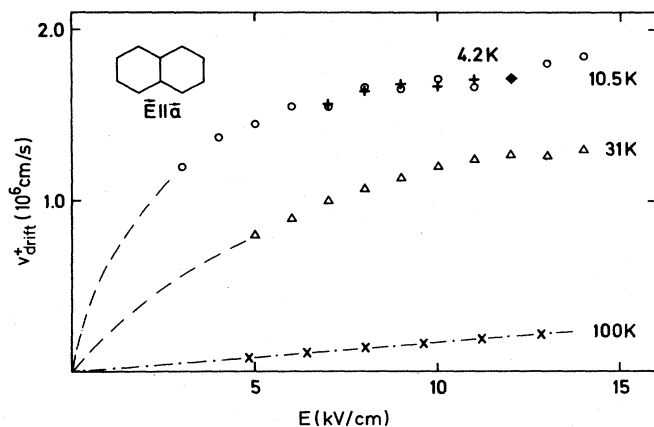


FIG 3. Hole drift velocity ( $v_N$ ) plotted as a function of the applied electric field for four different temperatures. The dashed and dotted line through the 100-K experimental points and the origin represents Ohm's law ( $v \propto E$ ); the dashed extrapolations of the 31- and 10.5-K points are a guide to the eye, indicating a strongly sublinear (sub-Ohmic)  $v(E)$  dependence. (This figure was presented at the 10th Molecular Crystal Symposium, 20–24 Sept. 1982, St. Jovite, Canada, in a post-deadline poster.)

the temperature to 4.2 K does not appreciably increase the charge-carrier velocity any further at any given field (in the experimentally accessible field range and within the experimental error limits). This saturation behavior was confirmed by measurements of the electric field dependence at several other temperatures between 12 and 4.2 K that were not plotted in the figure.

#### IV. DISCUSSION

In what follows we will derive arguments to show that the high, field-dependent hole mobilities observed in naphthalene at low temperatures can be understood in the framework of a standard wide-band-theory description. Wide-band theory has commonly been used for explaining electric-field-dependent mobilities in conventional inorganic semiconductors. In  $n$ -type germanium the phenomenon of electric field dependence of charge-carrier mobilities (first observed by Shockley and Ryder<sup>18</sup>) was attributed to a decrease of the momentum relaxation time for acoustic-phonon scattering with rising carrier energy. Since then, hot-electron phenomena have been extensively investigated in germanium and in several other inorganic semiconductors (see, e.g., Refs. 19 and 20). Influences on the drift velocity by acoustic- and optical-phonon scattering, impurity and intervalley scattering, and nonparabolicity of the band structure, acting both separately and in combination, have been considered.<sup>21–25</sup> Monte Carlo calculations for germanium, e.g., taking into account all these different mechanisms, were able to reach a quantitative fit to the experimental points.<sup>26</sup> This success was based on the availability of precise experimental data on the relevant material parameters, especially on the band structure.

Not only are there no such data available for any organic photoconductor, but it was frequently questioned whether band theory was applicable at all, or if one of a

number of different hopping models would be more appropriate; see, for instance, Ref. 27. General reviews of transport models which have been developed for, or adapted to, molecular crystals may be found in the literature.<sup>28–30</sup> All attempts made so far to calculate the correct magnitudes and temperature dependences of the anisotropic charge-carrier mobilities in organic photoconductors have essentially failed. Among other things, this seems to be mainly due to the lack of knowledge of the band-structure parameters. In contrast to conventional semiconductors, it has not been possible to derive the charge-carrier band-structure parameters for organic photoconductors from direct experimental results. Optical methods, for example, failed because of the occurrence of strong excitonic transitions in the spectral region about the band-gap energy. The low symmetry and large number of atoms in the unit cell of aromatic hydrocarbons, on the other hand, have so far prohibited exact theoretical calculations of excess carrier band structures from first principles. Up to now, only one-electron Hückel calculations have been numerically tractable.<sup>31</sup> It seems questionable whether these numerical results reflect the real band structures. This point will be discussed later in the context of Sec. IV C. Generally, the calculated bandwidths are on the order of 10–100 meV. These values are not decisive enough to strongly support nor invalidate the applicability of wide-band transport theory to organic molecular crystals.

We will therefore consider in the first part of the following discussion the different relevant transport models. We will take as a prime criterion for the applicability of any of these models to the charge-carrier transport in naphthalene its ability to reproduce the steep temperature dependence of the hole mobility  $\mu \propto T^{-2.9}$  and, simultaneously, the weaker  $\mu \propto T^{-1.4}$  dependence of the electron mobility, found experimentally.

Under this criterion, hopping models are excluded in Sec. IV A. In Sec. IV B special band-theory approaches, developed specifically for organic molecular crystals, will be discussed, and it will be argued that, in their present state of development, they are not applicable either.

We will then demonstrate that classical wide-band theory can reproduce the observed temperature dependences. We will therefore base the discussion of the field dependence on this theory (Sec. IV C) and focus on the two major sources which can be responsible for a field dependence of the mobility in a standard band-type description: energy-dependent charge-carrier relaxation time (Sec. IV C 1) and nonparabolicity of the band structure (Sec. IV C 2).

Finally, in Sec. IV D we will check the self-consistency of the application of wide-band theory to mobilities in naphthalene. We shall conclude that this kind of description is self-consistent in the lower-temperature regime, but definitely not at room temperature, where several conceptual problems arise which cannot yet be solved.

##### A. Exclusion of hopping models

Hopping motion of localized charge carriers occurs when thermal fluctuations of energy levels and/or transfer integrals are large compared with the electronic exchange interaction. Hopping motion is conceptually not compati-

ble with the observed high mobilities, which increase strongly with decreasing temperature. Under different sets of assumptions (linear and quadratic, strong and weak phonon coupling, adiabatic and nonadiabatic limits in high- and low-temperature approximations) the resulting temperature dependence is always of the general form

$$\mu(T) \propto T^n \exp(-E_a/k_B T), \quad (1)$$

which is formally a combination of a band term (dominating the high-temperature behavior) and a localization factor (governing transport at low temperatures). In current models,  $n$  attains a value not exceeding  $-1.5$ .<sup>32</sup> The (formal) activation energy  $E_a$  contains parameters such as polaron binding energies, transfer integrals, and phonon energies, depending on the specific approach. A temperature-activated behavior at low temperatures is therefore characteristic of hopping motion, a situation which is not observed in the measurements presented here. Other approaches taking into account off-diagonal disorder<sup>33-36</sup> were specifically designed to explain almost-temperature-independent  $c^*$  mobilities<sup>9</sup> and thus do not apply here.

From a simple argument hopping mobilities are expected to rise with the electric field  $E$ : The potential energy developed by the field across a lattice distance lowers the depth of the potential well that localizes the charge carrier. A more elaborate polaron-hopping description by Austin<sup>37</sup> takes into account that the electric field cannot only increase, but can also decrease, hopping mobilities, by decreasing the energy-level coincidence probability. For a polaron with binding energy  $E_p$  (and an activation energy  $E_a = E_p/2$ ) on a linear chain with lattice distance  $a$ , the field dependence of the hopping mobility is predicted as

$$\mu(E, T) = \mu(E=0, T) \exp\left[-\frac{e^2 a^2 E^2}{8E_p k_B T}\right] \frac{\sinh(eaE/2k_B T)}{eaE/2k_B T}. \quad (2)$$

A numerical fit of this calculated dependence to the experimental  $\mu(E)$  results at 31 K could only be (approximately) obtained with  $E_p < 0.1$  meV. A fit of the data at the lower temperatures would require still smaller polaron binding energies,  $E_p \ll k_B T$ , invalidating the polaron approach. Therefore the dependences of the hole mobilities in naphthalene on both temperature and electric field exclude the possibility that transport is by hopping.

#### B. Are there possible band-model approaches?

*Polaron band transport* has been described by Holstein in his pioneering paper on small polarons,<sup>38</sup> using basic concepts in a one-dimensional model. He derived the small-polaron band mobility as

$$\mu(T) = \frac{ea^2}{k_B T} 2\omega \left[ \frac{\alpha}{\pi} \operatorname{csch}\left[\frac{\hbar\omega}{2k_B T}\right] \right]^{1/2} \times \exp\left[-2\alpha \operatorname{csch}\left[\frac{\hbar\omega}{2k_B T}\right]\right], \quad (3)$$

where  $\alpha = E_p/\hbar\omega$  is the ratio of the polaron binding energy  $E_p$  to a characteristic optical-phonon energy  $\hbar\omega$ , and

thus represents the electron-phonon-coupling strength. In the range of validity of Holstein's model, this theoretical temperature dependence is a strongly decreasing function of temperature. Our experimental results could be fitted with expression (3) only with the assumption of a weakly bound polaron ( $E_p < 10$  meV) with very weak coupling strength ( $\alpha < 1$ ). For these parameters the model<sup>38</sup> predicts a band-to-hopping transition at  $T \leq 50$  K associated with a sharp change from a decreasing to a rising temperature dependence with increasing temperature, in contrast to experiment. Moreover, the parameter  $\alpha$ , which would be necessary to obtain a fit, definitely lies outside the limits of applicability of Holstein's model. Polaron band motion, as used in the above formalism, is therefore not suited to explain our experimental results.

Holstein and most other authors assumed that the charge carrier is sufficiently localized for being completely dressed with phonons. We cannot exclude, however, that *partial* polaron formation takes place (leading to only partial polaron band narrowing) and is reflected in the mobility. However, there is no comprehensive calculation for this situation available. The only treatment in the literature (Vilfan<sup>32</sup>) results in  $\mu \propto T^{-1.5} \exp(-E_a/k_B T)$ , i.e., a pure bandlike behavior at high temperature, and a simple temperature-activated hopping at low temperature. In the experiment, however, no temperature activation is observed, so that also within this model no indication of polaron formation can be concluded from the experiment.

It might be expected that *other narrow-band-theory approaches* conceived for low-mobility materials would provide a promising access to an understanding of the present results. However, it appears that these models are still less developed than those for wide-band semiconductors. In particular, hot-electron phenomena either have not or have not been adequately discussed. (This deficiency is probably due to the fact that there was no experimental evidence for fast carrier motion at low temperatures for the class of materials which exhibit small mobilities at high temperatures.) Other temperature-dependent narrow-band calculations have been compiled, e.g., by Schein.<sup>39</sup> Several important approaches will be discussed subsequently.

Friedman<sup>40</sup> derived, for acoustic-phonon scattering in one dimension, a  $\mu \propto T^{-2}$  dependence for a bandwidth  $W < k_B T$ , which changes to about  $T^{-3}$  for  $W > k_B T$ . Although these temperature dependences are similar to those found experimentally for holes in naphthalene, the smaller exponent of the temperature dependence of the electron mobility cannot be explained with this model. More seriously, there appears to be a discrepancy between the wide-band *limit* in Friedman's model ( $\mu \propto T^{-3}$ ) and the conventional result,  $\mu \propto T^{-1.5}$  (well established in the classical theory for wide-band semiconductors with acoustic-phonon scattering).

Sumi assumes in his model<sup>33,34</sup> a band motion in two dimensions ( $a$ - $b$  plane) with acoustic-phonon scattering. He predicts a  $\mu \propto T^n$  dependence, with  $n = -1.5$  for temperatures above the Debye temperature  $\Theta_D$ ;  $|n|$  increases to  $|n| > 2$  for lower temperatures. In naphthalene,  $\Theta_D \sim 200$  K,<sup>41</sup> and therefore a steeper rise of  $\mu$  with decreasing temperature should be visible in the ex-

perimental data; the experimental temperature dependence of the electron mobilities, however, exhibits a uniform exponent of  $n = -1.4$  in the entire temperature range above and below the Debye temperature; cf. Fig. 2. Predictions of a field dependence of the mobilities are discussed by Sumi only for the (slow) electrons in the  $c^*$  direction. However, Sumi ascribes transport in this special situation (almost temperature-independent electron mobility) to a hopping motion with increasing band contribution with decreasing temperature. In this model he derives a field dependence which has been neither confirmed experimentally<sup>13</sup> nor applies to the other crystallographic directions.

Silbey and Munn<sup>42</sup> formulated a very general approach: Starting from a model Hamiltonian, this approach has been devised to describe the intermediate range between free band motion and transport by polarons. The present level of elaboration, however, gives exact results only for the limits of a wide band on one hand or a fully dressed polaron on the other. An exact solution in the intermediate range, of interest here, was not obtained, but the authors state that there would be qualitative similarity between the exact expressions and their approximate ones. These approximate expressions allow the extension of Holstein's strong-coupling limit to the case of a weakly coupled polaron. If we compare our experimental results to these model calculations, a similar temperature dependence can be obtained only if we assume a *very weak* electron-phonon coupling. This implies that the transport behavior in naphthalene ( $a$  direction) comes close to the classical wide-band limit. However, the Silbey-Munn model can only qualitatively account for a possible residual polaronic contribution. This is due to the assumption of a single phonon and a single coupling constant to describe the formation of the polaron and its scattering, and to the stringent omissions made in the derivation. Moreover, since the Silbey-Munn model describes the charge-carrier transport in terms of the diffusion constant in a thermal-equilibrium situation, it does not allow derivation of an electric field dependence of the mobility.

Since none of the models designed specifically for weakly interacting systems (such as molecular crystals) can describe our results, we must confine the following discussion to predictions made by standard wide-band semiconductor theory. First, we will demonstrate that this theory is in fact able to describe the observed temperature dependences.

Acoustic deformation-potential scattering with equipartition of energy among the lattice oscillators leads to the familiar  $\mu_{ac}(T) \propto T^{-1.5}$  dependence. Our experimental results for the electron mobilities are compatible with this temperature dependence (a fact which has also been commented on recently by Anderson *et al.*<sup>43</sup>). For combined acoustic and optical deformation-potential scattering the theoretical temperature dependence changes to  $\mu(T) = \mu(T)f(T)$  (see, e.g., Ref. 20), where the additional factor  $f(T)$  depends very sensitively on the optical-phonon energy (and on the ratio of the coupling strengths of the charge carriers to both phonon types). If this additional temperature dependence in  $f(T)$  is strong enough, combined acoustic- and optical-phonon scattering can lead to a rather steep temperature dependence and thus

explain  $\mu \propto T^{-2.9}$ , observed for the naphthalene hole mobilities. This requires optical-phonon energies well above  $k_B T$  (and, in addition, strong coupling). Normally in organic molecular crystals the energies of intermolecular phonons are below room-temperature thermal energies (the highest optical-phonon mode in naphthalene is equivalent to 200 K).<sup>44</sup> Therefore intramolecular phonons ("vibrons") must be involved. It is worth mentioning that an interpretation with (additional) optical-phonon scattering has been used in the literature, e.g., for explaining the steep temperature dependence of the hole mobility in Ge,  $\mu \propto T^{-2.3}$ , cf. Ref. 19.

However, in a description based on band transport there exists an additional mechanism which can contribute to a faster decline of the mobility with increasing temperature. Band calculations suggest fairly small bandwidths for naphthalene and similar compounds (see, e.g., Ref. 31). In materials with narrow bands the thermal energy of the charge carriers can be sufficient to populate higher band states. The band shape in these higher states can be expected to be strongly nonparabolic, leading to an increase of the effective mass of the carriers above the value in the parabolic region at the bottom of the energy band. The increase of the average effective mass with increasing temperature would thus cause an additional decrease of the mobility; the temperature dependence would then become steeper than expected from the scattering mechanisms alone. In  $p$ -type Si, for instance, this effect was found to play a major role,<sup>45,46</sup> which is due to the fact that in this material the energy-band shape is already strongly nonparabolic at low carrier energies. The observed  $\mu \propto T^{-2.8}$  dependence was reproduced in a calculation which took into account acoustic- and optical-phonon scattering and band nonparabolicity.

In comparison, it is reasonable to assume that the low-temperature charge-carrier transport in naphthalene is also governed by these principal mechanisms. We will now demonstrate that, in fact, the mechanisms, which can in principle reproduce the experimental *temperature dependences* of the mobilities in naphthalene in a band-model description, can also account for the observed *field dependence* of the hole mobility at low temperatures.

### C. Field dependence of mobilities compatible with the band model

#### 1. Field dependence due to energy-dependent relaxation times

In the following paragraph we will assume a parabolic band and first discuss scattering of hot charge carriers by acoustic-, and then by optical-phonon modes. For both cases the results given here were first derived by Shockley.<sup>18</sup> For the former case it is assumed that the energy distribution of the hot carriers can be described by an energy-randomized Maxwell-Boltzmann distribution at a carrier temperature  $T_e$  higher than the lattice temperature  $T$ . Furthermore, equipartition of thermal energy among the phonon states and a parabolic charge-carrier energy band are assumed. A standard perturbation-theory calculation of the momentum relaxation time  $\langle \tau_{m,ac} \rangle$ , treating

acoustic-phonon scattering in the deformation-potential approximation, then leads to (cf. Ref. 20)

$$\langle \tau_{m,ac} \rangle = \frac{4}{3\sqrt{\pi}} l_{ac} (2\varepsilon/m^*)^{-1/2}, \quad (4)$$

where

$$\varepsilon = k_B T_e,$$

and

$$l_{ac} = \frac{\pi^{3/2} \hbar^4 \rho u_L^2}{2m^*{}^2 E_{ac}^2 k_B T}$$

is the charge-carrier mean free path in the case of elastic scattering,  $u_L$  is the longitudinal sound velocity,  $\rho$  is the mass density, and  $E_{ac}$ , the deformation-potential constant, is the shift of the band edge per unit relative lattice dilation. If with increasing field the charge-carrier temperature  $T_e$  rises above the thermal-equilibrium value  $T$ ,  $\langle \tau_{m,ac} \rangle$  decreases continuously ( $\langle \tau_{m,ac} \rangle \propto T_e^{-1/2}$ ).

Using this result, the dependence of  $\mu$  on the electric field  $E$  is obtained as follows: The charge-carrier temperature  $T_e$  is established by the balance between energy gain from the field  $e\mu(T_e)E^2$  and energy loss to phonons per unit time, where  $\mu(T_e)$  is obtained from  $\langle \tau_{m,ac} \rangle$  at  $T_e$ , Eq. (4). Finally, an expression for  $\mu(E)$  and, hence, for  $v_d(E) = \mu(E)E$ , results<sup>18</sup>

$$v_d(E) = \mu_0 E \sqrt{2} \left\{ 1 + \left[ 1 + \frac{3\pi}{8} \left( \frac{\mu_0 E}{u_L} \right)^2 \right]^{1/2} \right\}^{-1/2} \quad (5)$$

(where the positive roots must be taken).

In this approach the field dependence of the drift velocity  $v_d(T, E)$  is determined solely by the speed  $u_L(T)$  of longitudinal lattice waves and the small-field Ohmic mobility  $\mu_0(T)$ . Because of scattering, a certain directional average of the anisotropic sound velocity must be taken. Reliable numbers of the anisotropic sound velocities can be obtained from the phonon dispersion curves, which were measured by inelastic neutron scattering for naphthalene- $d_8$ .<sup>41</sup> Theoretical considerations suggest that in naphthalene- $h_8$  the sound velocities are higher by a factor of the ratio of the molecular masses  $136/128 = 1.06$ , cf. Ref. 47. We take  $4 \times 10^5$  cm/s for the average  $u_L$  at 6 K and use an extrapolation into the low-temperature (field dependence) regime of the high-temperature Ohmic  $\mu_0 \propto T^n$  dependence to estimate  $\mu_0$  at low temperatures. Curves  $v_d(E)$  calculated with this model for different temperatures are compared with the experimental points in Fig. 4.

For 35 K a close fit is obtained. However, at 31 K the measured velocities fall below the predicted curves for electric fields  $E > 10$  kV/cm. At still lower temperatures, e.g., at 19 K, the fitting curve required the (not unreasonable) assumption of a decrease of the exponent  $n$  below the value extrapolated from the higher-temperature region, leading to  $\mu_0(19 \text{ K}) = 420 \text{ cm}^2/\text{Vs}$  instead of  $490 \text{ cm}^2/\text{Vs}$  (resulting from the  $T^n$  extrapolation). However, the saturation behavior of  $v_d$  below  $\sim 10$  K (see Fig. 3) cannot be reproduced at all with this type of acoustic-phonon scattering, which always leads to a rise  $v_d \propto \sqrt{E}$ .

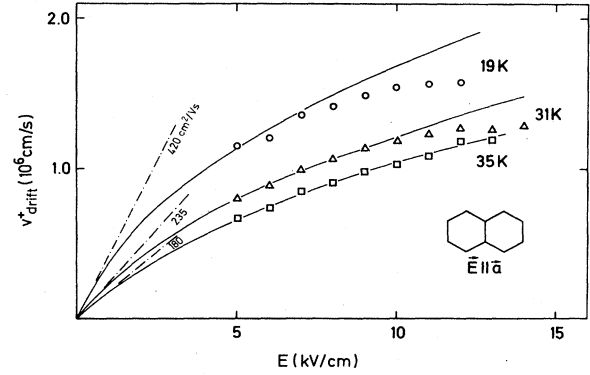


FIG. 4. Hole drift velocity  $v_N$  plotted as a function of the applied electric field for 35, 31, and 19 K. The solid lines are a fit to the experimental points by Eq. (5), describing acoustic-phonon scattering of hot electrons in a deformation-potential approximation (with the sound velocity  $u_L = 4 \times 10^5$  cm/s). The slopes of the dashed and dotted tangents represent the low-field Ohmic mobilities  $\mu_0$  used in the model.

(A weaker dependence could be due to a violation of the equipartition condition, but this is not considered to be prominent here.)

It is in fact surprising that this basic "electron temperature model" that we have used so far can indeed quantitatively account for the first deviations from Ohmic behavior, if one considers (among other approximations) that the effect of the complicated anisotropic electron-phonon interaction has been reduced to a single number (the average sound velocity) and that the real anisotropic band structure has been represented by an isotropic parabolic  $\varepsilon(k)$  dependence. On the other hand, calculated  $v(E)$  curves that at least partially fit the measured ones can indeed only be obtained in a very narrow range of the fit parameters  $\mu_0$  and  $u_L$  near the experimentally relevant values. This fact strongly supports the applicability of this description, which is strictly based on band-model calculations. Since the derivation of Eq. (5) uses an energy-randomized Maxwell-Boltzmann distribution, it is valid only for small deviations from thermal equilibrium, but not for situations in which the charge carriers gain much more energy from the field than  $k_B T$ .

We will now consider two prominent mechanisms which are able to describe hot carrier dynamics near the limit of *saturated drift velocities*, namely relaxation by optical-phonon emission and nonparabolicity of the band structure. Depending on the maximum energy to which a charge carrier can be brought by the electric field (an energy, which, for a certain observed saturation velocity, depends on the effective mass), either one of these two mechanisms will be dominant. It is easy to understand, how *emission of optical phonons* can account for a saturation of the drift velocity, if one uses a simple argument, which also was given by Shockley<sup>18</sup> in 1951 [the same picture has frequently been applied to classical semiconductors such as GaAs (Ref. 48) and silicon (Ref. 49)]. In this picture the carrier is assumed to be freely accelerated according to  $m^* \dot{v}_d = eEt$ , thereby increasing its momentum

linearly with time,  $\hbar k = eEt$ , until finally, it has gained enough energy from the electric field to generate an optical phonon of energy  $\hbar\omega$  at a certain time  $\tau$ , where

$$\varepsilon(k(\tau)) = \frac{[\hbar k(\tau)]^2}{2m^*} = \hbar\omega. \quad (6)$$

The cyclic repetition of this acceleration process leads to an average field-independent drift velocity,

$$v_{d,s} = (\hbar\omega/2m^*)^{1/2}. \quad (7a)$$

This picture implies a highly anisotropic carrier momentum distribution (equivalent to a "streaming" motion along the field direction), and is therefore quite different from the thermal-equilibrium situation (Boltzmann distribution at an elevated carrier temperature  $T_e$ ), which was assumed in the treatment of acoustic-phonon scattering above. It is appropriate to consider both approaches since the latter is suited to describe initial deviations from Ohmic mobility at higher temperatures (but is inappropriate for dominating optical-phonon scattering), whereas the former case is useful for understanding the final saturation of drift velocities at high electric fields and low temperatures (where the "streaming" motion is no longer thermally randomized).

But the calculated saturation value is not very sensitive to the detailed assumptions made for the carrier distribution. Even the use of a Maxwell-Boltzmann distribution at  $T_e$  in a model of optical deformation-potential scattering (which is a good approximation only for  $k_B T_e \gg \hbar\omega$ ) (cf. Ref. 20) adds only a weak temperature dependence and a small numerical factor to the result obtained above:

$$v_{d,s} = [3\hbar\omega/4m^* \coth(z)]^{1/2} \quad \text{where } z = \hbar\omega/2k_B T. \quad (7b)$$

For  $2k_B T \ll \hbar\omega$ , which is the case for naphthalene below 10 K,  $\coth(z) \rightarrow 1$ , and  $v_{d,s}$  should become temperature independent. This behavior is in fact observed (cf. Fig. 3). From the experimental value of the charge-carrier saturation velocity,  $v_{d,s} = 1.8 \times 10^6$  cm/s, and the lowest optical-phonon energy,  $\hbar\omega = 6.9$  meV,<sup>44</sup> an effective hole mass of  $m^* \sim 3m_e$  can be calculated with Eq. (7b).

## 2. Effects of a nonparabolic band structure

Throughout the preceding subsection a band structure was used which was assumed to be parabolic, at least up to the lowest optical-phonon energy. This assumption can be justified if the effective mass is indeed as small as estimated above ( $m^* \sim 3m_e$ ). Then at the maximum observed drift velocity the carrier reaches only a value corresponding to a  $k$  vector with  $|k| \sim 5 \times 10^6$  cm<sup>-1</sup>, which is small compared to the Brillouin-zone boundary calculated from the largest lattice constant of naphthalene,  $k_{\max} = 3.7 \times 10^7$  cm<sup>-1</sup>. On the other hand, the above argument was based on the assumption that the electron energy cannot exceed the optical-phonon energy  $\hbar\omega$  (due to strong generative scattering). Equations (7a) and (7b) apply only to this case, and only then does the observed saturation velocity lead to the small effective mass  $m^* = 3m_e$ , which is consistent with the use of a parabolic band structure. However, since we have, in fact, no

knowledge of the effective mass, assuming a higher value of  $m^*$  would still be consistent with the observed high drift velocities, if the optical-phonon interaction was much less efficient. Then the electron energy,  $\varepsilon = m^* v_d^2/2$ , can exceed the lowest optical-phonon energy, and the observed (saturation) drift velocity would imply a higher effective mass, correlated with a smaller bandwidth. Consequently, at high fields the carriers would reach energy-band regions with strongly increasing effective mass, and the drift velocity would ultimately be limited by the maximum speed which is possible in the band.

We will now briefly outline how a nonparabolic energy band would affect the carrier velocity; we assume a simple model, similar to that used in the discussion of optical-phonon scattering. However, we now take a cosine-shaped band

$$\varepsilon(k) = \text{const} - \frac{1}{2} W \cos(\mathbf{k} \cdot \mathbf{a}) \quad (8)$$

of width  $W$ ; a single charge carrier starting with  $k=0$  at the center of the Brillouin zone is again assumed to increase its momentum  $\hbar k$  linearly with time before it is scattered back to  $k=0$  at a certain collision time  $\tau$ . At this moment it has reached a velocity

$$v(\tau) = \frac{1}{\hbar} \frac{\partial \varepsilon}{\partial k} \Big|_{k(\tau)} = \frac{Wa}{2\hbar} \sin \left[ \frac{eaE}{\hbar} \tau \right]. \quad (9)$$

If we assume further that  $\tau$  is sufficiently small, so that  $k$  does not reach the zone boundary, we find, for the average velocity between times 0 and  $\tau$ ,

$$\bar{v}(E, \tau) = \frac{Wa}{2\hbar} \left[ 1 - \cos \left[ \frac{eaE}{\hbar} \tau \right] \right] \left[ \frac{eaE}{\hbar} \tau \right]^{-1}. \quad (10)$$

Expanding the cosine for small fields, we recover the usual Ohmic behavior  $\bar{v} = \mu E$ , with  $\mu = (e/m^*)\tau$ . At high fields,  $\bar{v}(E)$  tends toward a saturated average drift velocity  $\bar{v}_{\max} = 0.724 Wa/\pi\hbar$ , which is determined only by the bandwidth. In naphthalene, in the  $a$  direction, this limitation of the velocity by the band shape would be sufficient to explain the observed saturated hole drift velocity, if we assumed a width of the valence band of  $W \sim 40$  meV. The most elaborate model calculations presently available in the literature<sup>31</sup> give the widths  $W$  for a carrier with its  $k$  vector parallel to the crystallographic  $a$  direction as 30 meV. This coincidence might be taken as confirmation that the limitation of the drift velocity is in fact given by the bandwidth. However, since the band structures for complex organic crystals can be calculated only with severe approximations, this agreement appears rather fortuitous. This suspicion is further supported by the gross qualitative disagreement between the anisotropy of the valence-band widths in the  $a$  and  $c^*$  directions calculated in Ref. 31 as  $W_a:W_{c^*} = 1:5$  (suggesting that the mobility in the  $a$  direction should be much smaller than that in the  $c^*$  direction), and the measured room-temperature mobility values: In contrast to the prediction in Ref. 31,  $\mu_{aa} = 0.94$  cm<sup>2</sup>/V s is much higher than  $\mu_{c^*c^*} = 0.32$  cm<sup>2</sup>/V s;<sup>17</sup>  $\mu_{aa}:\mu_{c^*c^*} = 2.9:1$ .

In summary, we have demonstrated, for naphthalene, that the observed non-Ohmic charge-carrier drift velocities at low temperatures can be explained in a standard

band-transport model. To arrive at a decisive conclusion as to which of the different mechanisms (which can be effective within a band approach) contributes to what extent, reliable information about the underlying band structure would be needed first.

Even with knowledge of the band structure, a complete quantitative explanation of the experimental data using combined acoustic- and optical-phonon scattering in non-parabolic bands is a complicated computational problem. It is not possible to calculate the relaxation time due to one scattering mechanism without taking into account the other, because the actual carrier temperature  $T_e$  is determined by the energy loss to both channels. (This problem has been treated in the past by Monte Carlo simulations, e.g., for germanium in Ref. 26.)

#### D. Consistency of the band picture

In this subsection we will check if the application of the standard band-transport model to naphthalene is self-consistent. We will especially check if the criterion (discussed extensively, e.g., in Ref. 27) that the coherence length of the electron wave packet, characterized by the mean free path  $\lambda$ , exceeds a lattice distance  $a$ , is fulfilled. If so, the use of extended Bloch states to describe the charge carriers in a band picture would be justified (see, e.g., Ref. 30).

For an order-of-magnitude estimate, we define  $\lambda$  simply by  $\lambda = v\tau$ , taking for  $v$  the thermal velocity  $v_{th} = (3k_B T/m^*)^{1/2}$  and for  $\tau$  a mean free time between collisions which (under the assumption of effective momentum relaxation) we deduce from the observed mobility  $\mu$  as  $\tau = \mu m^*/e$ . The mean free path then becomes

$$\lambda = (\mu/e)(3m^*k_B T)^{1/2}. \quad (11)$$

For a certain mobility at a certain temperature,  $\lambda$  depends only on the effective mass. We will therefore derive several estimates for the effective mass from the different approaches which we previously used in the discussion of the field dependence at low temperatures.

The successful application of the acoustic deformation-potential-scattering model for explaining the field dependence at 35 K sets an approximate upper limit for  $m^*$ : In this model it must be assumed that we can define a charge-carrier temperature  $T_e$ ; this requires a distribution function of the form  $f = f_0(\epsilon, E) + f_1$  (with  $f_0$  depending only on the randomized carrier energy  $\epsilon = 3k_B T_e/2$ , and a term  $f_1$  depending on the drift velocity vector).  $f_1$  must be much smaller than  $f_0$ . This implies that the kinetic energy  $\epsilon_d = m^* v_d^2/2$  contained in the drift motion of the carriers should be considerably smaller than the thermal energy  $\epsilon_{th} = k_B T/2$  contained in the diffusion motion parallel to the field. This condition sets an upper limit on the possible range of the effective masses at  $m^* \sim 15$  [for  $\epsilon_{th} > 3\epsilon_d$ , and  $v_d = 1.2 \times 10^6$  cm/s at 31 K, the highest value describable by the acoustic-phonon-scattering model used in the derivation of Eq. (5)]. For an explanation of the saturation of the drift velocity based on optical-phonon emission,  $m^* \sim 3m_e$  has been derived above.

Conversely, if the valence band was much narrower

than what would be expected for an effective mass  $m^* = 3m_e$ , the holes would reach energy states in which increasing effective mass would finally control their velocity. Then, for an exact evaluation of the average effective mass, knowledge of the exact carrier distribution (determined by the inelastic scattering with short-wavelength phonons) over the strongly curved energy band would be required. For this case we will assume, as a lower limit, that value of  $m^*$  which is obtained at  $k=0$  for a cosine-shaped band with  $W=40$  meV (as derived in Sec. IV C 2):

$$m^*(k=0) = \hbar^2 \left[ \frac{\partial^2 \epsilon}{\partial k^2} \right]^{-1} \Big|_{k=0} = \frac{2\hbar^2}{W a^2} \approx 6m_e. \quad (12)$$

For these limits of the range of possible effective hole masses ( $3m_e < m^* < 15m_e$ ), an estimate of the range of the mean free paths  $\lambda$  can be obtained by using Eq. (11). At 40 K, with  $\mu \sim 90$  cm<sup>2</sup>/Vs, we arrive at a mean free path of approximately five lattice constants ( $m^* = 3m_e$ ) or more ( $m^* > 3m_e$ ). At 19 K the measured mobility was already limited by the field, even for the lowest useful field.  $\mu_0 > \mu(E) = 240$  cm<sup>2</sup>/Vs is therefore a lower limit for the Ohmic mobility and  $\lambda$  is at least eight lattice constants. These mean free paths definitely support the band-model description for the low-temperature mobilities.

However, with the effective masses that we estimated from the high mobilities at low temperature, a consistent band description of the low *room-temperature* mobilities cannot be achieved, not even with the highest estimated value,  $m^* = 15m_e$ . The calculated mean free path  $\lambda$  turns out to be much smaller than a lattice constant. This inconsistency might suggest a different transport mechanism at higher temperatures. However, it would not be easy to understand why a change in the transport mechanism should not be associated with an observable change in the temperature dependence; but the temperature dependence of  $\mu$  is unchanged from the low-temperature high-mobility regime to the high-temperature low-mobility regime. We therefore propose the following conditions, which might allow an extension of the band approach to higher temperatures.

If the width of the valence band is in fact only 40 meV, as we estimated above for the case of drift-velocity limitation by the bandwidth, then at high temperatures a large fraction of the carriers reaches states with higher effective mass; therefore the apparent average value of the effective mass increases greatly with increasing temperature. The value of  $m^* = 6m_e$  derived above for the lower, parabolic, band region (solely populated at low temperatures) could eventually rise to a value sufficiently high for self-consistency of the band picture even at high temperatures. Alternatively, we may attribute the small room-temperature mobilities to partial polaron formation at higher temperature. In this case the wide bands at low temperature would become much smaller at higher temperatures due to exponential band narrowing with rising temperature. Both approaches are also compatible with the observed steep temperature dependence of the hole mobilities (see Sec. IV B).

These suggestions, however, cannot easily be used to explain the *electron* mobilities as well. The electrons behave in a manner similar to the holes in that they reach fairly high mobility values at low temperatures; these values are still consistent with a band-model description. However, their temperature dependence  $\mu_{aa}^- \propto T^{-1.4}$ , well understood as such in a wide-band-transport model with acoustic-phonon scattering, cannot easily be reconciled with the small room-temperature mobility value,  $\mu(290\text{ K}) = 0.63\text{ cm}^2/\text{Vs}$ . Following the above argument, an effective mass of almost  $400m_e$  would be required. This high value could be reached only if one of the two mechanisms discussed above for the holes would apply to the electrons as well. The temperature dependence of the electron mobilities, however, would then also be expected to become much steeper than  $\mu \propto T^{-1.5}$  (arising from acoustic-phonon scattering alone), in contradiction to the experimental result.

## V. CONCLUSION

In summary, we have observed hot charge carriers in the organic molecular crystal naphthalene for the first time. Toward low temperatures the mobilities become high and strongly electric field dependent. At the lowest temperatures the drift velocities tend to saturate. We have derived arguments that a classical band-type transport model is well suited for a consistent description of the observed dependences of low-temperature mobilities on temperature and electric field. In a band-model description both energy-dependent scattering and energy-dependent effective mass must be taken into account. On

the other hand, our results continuously span the range between these high band mobilities at low temperatures and the low mobilities at high temperatures, for which the band picture is barely consistent. Thus our data provide a new challenge for developing a general transport theory that is able to explain these *two* regimes and link them in a unified description.

*Note added in proof.* By using thinner samples it was possible to shift the field limitation in the crystal (by electric breakdown of the He heat-exchange gas) to higher fields since a field dependence of the electron mobility  $\mu_{aa}^-$  was observed too (for  $E \geq 14\text{ kV/cm}$  at 22.5 K). For samples with slightly other crystallographic orientations, electron transits could be obtained at still lower temperatures (down to 4.2 K), displaying pronounced field dependences of the mobilities even at much lower electric fields ( $E \gtrsim 5\text{ kV/cm}$ ).

## ACKNOWLEDGMENTS

We are greatly indebted to Professor Bob Munn of the University of Manchester Institute of Science and Technology, Manchester, U.K., for a critical reading of the manuscript; we also wish to thank him and Roland Stehle, Universität Stuttgart, for helpful discussions. The naphthalene crystals were purified and prepared by W. Tuffentsammer and M. Gerdon in our Crystal Laboratory (Kristalllabor des Physikalischen Instituts der Universität Stuttgart). Their skillful work is greatly appreciated. The excimer laser was kindly placed at our disposal by Professor M. Pilkuhn and co-workers. This work was supported by the Deutsche Forschungsgemeinschaft.

<sup>1</sup>R. G. Kepler, Phys. Rev. **119**, 1226 (1960).

<sup>2</sup>O. H. LeBlanc, Jr., J. Chem. Phys. **33**, 626 (1960).

<sup>3</sup>L. M. Schwartz, H. G. Ingersoll, Jr., and J. F. Hornig, Mol. Cryst. **2**, 379 (1967).

<sup>4</sup>N. Karl, in *Festkörperprobleme (Advances in Solid State Physics)*, edited by H. J. Queisser (Pergamon/Vieweg, Braunschweig, 1974), Vol. 14, p. 261.

<sup>5</sup>K.-H. Probst and N. Karl, Phys. Status Solidi A **27**, 499 (1975).

<sup>6</sup>Z. Burshtein and D. F. Williams, Phys. Rev. B **15**, 5769 (1977).

<sup>7</sup>N. Karl and W. Warta (unpublished).

<sup>8</sup>R. Stehle and N. Karl, presented at the 3rd Conference on Electrical and Related Properties of Organic Solids, Wdzydze Kiszewskie, Poland, 1981, as a post-deadline paper (unpublished).

<sup>9</sup>L. B. Schein and A. R. McGhie, Phys. Rev. B **20**, 1631 (1979); see also L. B. Schein, L. B. Duke, and A. R. McGhie, Phys. Rev. Lett. **40**, 197 (1978).

<sup>10</sup>L. B. Schein and A. R. McGhie, Chem. Phys. Lett. **62**, 356 (1979).

<sup>11</sup>S. Nakano and Y. Maruyama, Solid State Commun. **35**, 671 (1980).

<sup>12</sup>N. Karl, comment made, at the 9th Molecular Crystal Symposium, 1980 (unpublished).

<sup>13</sup>L. B. Schein, R. S. Narang, R. W. Anderson, K. E. Meyer, and A. R. McGhie, Chem. Phys. Lett. **100**, 37 (1983).

<sup>14</sup>N. Karl, in *Crystals, Growth, Properties and Applications*, edited by H. C. Freyhardt (Springer, Berlin, 1980), Vol. 4, pp. 1–100.

<sup>15</sup>N. Karl, J. Cryst. Growth **51**, 509 (1981).

<sup>16</sup>N. Karl, H. Port, and W. Schrof, Mol. Cryst. Liq. Cryst. **78**, 55 (1981).

<sup>17</sup>L. B. Schein, W. Warta, A. R. McGhie, and N. Karl, Chem. Phys. Lett. **100**, 34 (1983).

<sup>18</sup>W. Shockley, Bell Syst. Tech. J. **30**, 990 (1951).

<sup>19</sup>E. M. Conwell, *High Field Transport in Semiconductors* (Academic, New York, 1967).

<sup>20</sup>K. Seeger, *Semiconductor Physics*, 2nd ed. (Springer, Berlin, 1982).

<sup>21</sup>J. G. Ruch and W. Fawcett, J. Appl. Phys. **41**, 3843 (1970).

<sup>22</sup>W. Fawcett, D. A. Boardman, and S. Swain, J. Phys. Chem. Solids **31**, 1963 (1970).

<sup>23</sup>W. Fawcett and E. G. S. Paige, J. Phys. C **4**, 1801 (1971).

<sup>24</sup>T. J. Maloney and J. Frey, J. Appl. Phys. **48**, 781 (1977).

<sup>25</sup>W. Duhmke, Phys. Rev. B **2**, 987 (1970).

<sup>26</sup>L. Reggiani, C. Canali, F. Nava, and G. Ottaviani, Phys. Rev. B **16**, 2781 (1977).

<sup>27</sup>R. M. Glaeser and R. S. Berry, J. Chem. Phys. **44**, 3797 (1966).

<sup>28</sup>G. G. Roberts, N. Apsley, and R. W. Munn, Phys. Rep. **60**, 59 (1980).

- <sup>29</sup>M. Pope and C. E. Swenberg, *Electronic Processes in Organic Crystals* (Clarendon, Oxford, 1982).
- <sup>30</sup>S. D. Druger, in *Organic Molecular Photophysics*, edited by J. B. Birks (Wiley, London, 1975), Vol. II, p. 373.
- <sup>31</sup>D. C. Singh and S. C. Mathur, *Mol. Cryst. Liq. Cryst.* **27**, 55 (1974).
- <sup>32</sup>I. Vilfan, *Phys. Status Solid B* **59**, 351 (1973).
- <sup>33</sup>H. Sumi, *J. Chem. Phys.* **70**, 3775 (1979).
- <sup>34</sup>H. Sumi, *J. Chem. Phys.* **71**, 3403 (1979).
- <sup>35</sup>P. Reineker, V. M. Kenkre, and R. Kühne, *Phys. Lett.* **84A**, 294 (1981).
- <sup>36</sup>S. Efrima and H. Metiu, *Chem. Phys. Lett.* **60**, 226 (1979).
- <sup>37</sup>I. G. Austin and R. Gamble, in *Conduction in Low Mobility Materials*, edited by N. Klein, T. S. Tannhauser, and M. Polak (Taylor and Francis, London, 1971), p. 13.
- <sup>38</sup>T. Holstein, *Ann. Phys. (N.Y.)* **8**, 325 (1959); **8**, 343 (1959).
- <sup>39</sup>L. B. Schein, *Phys. Rev. B* **15**, 1024 (1977).
- <sup>40</sup>L. Friedman, *Phys. Rev. A* **140**, 1649 (1965).
- <sup>41</sup>I. Natkaniec, E. L. Bokhenkov, B. Dorner, J. Kalus, G. A. Mackenzie, G. S. Pawley, U. Schmelzer, and E. K. Sheka, *J. Phys. C* **13**, 4265 (1980).
- <sup>42</sup>R. Silbey and R. W. Munn, *J. Chem. Phys.* **72**, 2763 (1980); R. W. Munn, in *Physics of Dielectric Solids* (IOP, London, 1981), p. 98 (IOP Conf. Ser. No. 58).
- <sup>43</sup>J. D. Andersen, C. B. Duke, and V. M. Kenkre, *Phys. Rev. Lett.* **51**, 2202 (1983).
- <sup>44</sup>M. Suzuki, T. Yokoyama, and M. Ito, *Spectrochim. Acta* **24A**, 1091 (1968).
- <sup>45</sup>M. Asche and J. v. Borzeskovski, *Phys. Status Solidi* **37**, 433 (1970).
- <sup>46</sup>G. Ottaviani, L. Reggiani, C. Canali, F. Nava, and A. Alberigi Quaranta, *Phys. Rev. B* **12**, 3318 (1975).
- <sup>47</sup>R. Ostertag, Doktorarbeit, Universität Stuttgart, 1972.
- <sup>48</sup>L. F. Eastman, in *Festkörperprobleme XXII (Advances in Solid State Physics)*, edited by P. Grosse (Pergamon/Vieweg, Braunschweig, 1982), p. 173.
- <sup>49</sup>K. Kajita, *Solid State Commun.* **31**, 573 (1979).